Inkjet printing upconversion nanoparticles for anti-counterfeit applications

Minli You [a,b*], Junjie Zhong [b,c*], Yuan Hong [b,d], Zhenfeng Duan [e], Min Lin [a,b,e#], Feng Xu [a,b#]

Abstract:

Patterning upconversion luminescence materials has been widely used for anti-counterfeit and security applications, where a preferred method should be easy, fast, multicolor, high-throughput and designable. However, conventional patterning methods are complex and inflexible. Here, we report a digital and flexible inkjet printing based approach for producing high-resolution and high-luminescence anti-counterfeit patterns. We successfully printed different multicolor luminescent patterns by inkjet printing upconversion nanoparticles with controlled and uniform luminescence intensity through optimizing the inks and substrates. Combined with another downconversion luminescence material, we achieved two different patterns in the same area, which show up separately under excitation by different wavelength laser sources. The developed technology is promising to use one single subtract to carry abundant of information by printing multilayer patterns composed of luminescence materials with different excitation light.

Introduction

Anti-counterfeit technologies have found widespread applications in identity cards, currency, tags and important documents [1, 2]. These applications have shown significant importance for business and national public safety [3]. Especially with the rapid expansion of small business, sole traders and personal demands, there is an urgent need to develop a low cost, easy accessible, personalized anti-counterfeit technology. To meet this emerging need, various anti-counterfeit technologies including laser holography [4], nuclear track technology [5], luminescence printing [6] may be employed. Among which, luminescence printing offers several advantages such as high-throughput, designable and advanced anti-counterfeit performance. For luminescence-based anti-counterfeit, luminescence ink is used to produce various coded patterns and the anti-counterfeit property mainly results from two aspects, *i.e.*, the high concealment luminescence materials [7] and the complex coded pattern [8].

Both organic and inorganic luminescence materials based on a so-called 'downconversion' process (*e.g.*, photochromic compounds, semiconductor quantum dots, lanthanide doped oxides) have been used as luminescence ink [1, 9, 10], which are featured by longer-wavelength visible emission when exposed to shorter-wavelength excitation, mostly ultraviolet (UV) light. However, UV-to-visible downconversion materials and UV excitation sources have become more accessible, making it much easier to duplicate. In contrast, near-infrared (NIR)-to-visible luminescence materials based on so-called 'upconversion' luminescence are more difficult to duplicate as compared with UV-to-visible materials [11-17]. Besides, the NIR excitation sources are more difficult to access and will not excite standard downconversion luminescence materials, making it possible to print patterns on highly fluorescent surfaces (*e.g.*, papers and textiles with optical brighteners) [18]. Moreover, upconversion materials can be formulated to produce the designed emission color only under specific excitation power densities [19] and the designed luminescence lifetime by controlling the ratio of Yb and Tm [20, 21], making it even more difficult to duplicate.

To produce complicated, elaborate and high-resolution upconversion luminescence patterns for anti-counterfeit applications, various printing technologies have been explored. Kim *et al.* have fabricated predefined patterns of upconversion nanoparticles using a photolithography technique, which however involves multi-step process [14]. To simplify the operating process, Blumenthal *et al.* developed a one-step printing process accompanied by Sono-Tek screen-printing and M3D direct-write printing process based on NIR-to-visible inks composed of β-$NaYF_4$:Yb^{3+}, Er^{3+} nanoparticles in a polymer matrix [12]. This study was further extended by Meruga *et al.* for the fabrication of multicolor two-dimensional codes visible only under NIR excitation using a new one-step printing process based on Aerosol Jet technology [15, 16]. Although significant progress has been made, there are several limitations associated with these existing printing platforms. For example, screen-printer can only print one-color ink in a single printing process. Although aerosol jet printer holds high spatial resolution [12], it is time consuming and complex to operate due to its huge and intricate structure. In addition, poly (methyl methacrylate) (PMMA) is used as inks binding reagent to maintain film uniformity in these printing systems [12, 16]. This requires time-consuming procedure to prepare both inks and substrates. Besides, the use of PMMA in the ink involves the potential issue of 'coffee ring effect', which may result in fracture of printed patterns [12]. Therefore, developing an easy accessible, high-throughput, multicolor and designable printing method for upconversion-based anti-counterfeit applications is highly demanded.

To address above-mentioned challenges, we applied inkjet printing for patterning inks composed of upconversion nanoparticles. Inkjet printing is versatile and high-throughput, involves user-friendly processing steps. The inkjet printing has been widely used for fabrication of many complex structures, including transistor circuits [22-27], optical devices [28-33], chemical sensors [34-36], and so on. Their advanced applications can be attributed to the attractive features that include (1) the possibility for purely additive operation, in which corresponding inks are deposited only where they are needed, (2) the flexibility in choice of structure designs for producing complicated security patterns, where changes can be made rapidly through software-based printer-control systems (as shown in **Fig. 1**), (3) compatibility with large-area substrates and (4) the potential for high spatial resolution (depending on the DPI) and mass production [37]. These advantages render inkjet-printer as a prospective method for anti-counterfeit printing.

In this paper, we report the preparation of NIR-to-visible inks that is suitable for inkjet printing and multilayer patterns printing using luminescence materials with different excitation light. The developed method is capable of producing anti-counterfeit features with easy, fast, multicolor, high-throughput, designable and low cost. Essential characteristics of inks, substrates and the resulting patterns were studied. Contact angles between different inks and substrates were characterized to indicate the relationship with spatial resolution. In addition, luminescence intensity and uniformity were tested to prove the high quality of printed patterns. With the help of a personal computer, we produced different types of two-dimension patterns visible only under a 980 nm NIR excitation source. Furthermore, multilayer patterns were realized by printing an upconversion pattern (containing upconversion nanoparticles) over a downconversion pattern (containing downconversion dye). No background luminescence interference was observed on the overlap area, which increases the coding complex and is essential for security purposes.

Materials and Method

1. Materials

YCl_3 $6H_2O$, $YbCl_3$ $6H_2O$, $ErCl_3$ $6H_2O$, $TmCl_3$ $6H_2O$, Ammonium fluoride (NH_4F) were purchased from Sigma Aldrich. 1-Octacene (90%) Sodium and Oleic acid (90%) were obtained from Alfa Aesar. Methanol, Glycerol (99.0%), chloroform, ethanol and sodium hydroxide (NaOH) were obtained from Tianjinzhiyuan Chemical Reagen Co., Ltd. Poly (acrylic acid) was obtained from Tianjinyongsheng Chemical Reagen Co., Ltd. Glycerol trioleate (60%) was purchased from Aladdin Chemistry Co., Ltd. Sodium Dodecyl Sulfonate (SDS) (90%) was obtained from ChengDu Kelong Chemical Co., Ltd. All reagents except for Glycerol trioleate (chemically pure) were of analytical grade and were used without any purification. UV-Vis ink used here is #110UV Invisible Endorsing Noris Ink from NORIS USA Co., Ltd. Vegetable parchment was obtained from Suzhouguanhua Paper Factory. A4 duplicating paper was purchased from Double A (1991) Public Co., Ltd.

2. Synthesis of upconversion nanoparticles (UCNPs)

2.1 Synthesis of *β*-$NaYF_4$:Yb,Er/Tm Nanoparticles

UCNPs were synthesized following the protocol from literature [38]. In a typical synthesis of 30-nm sized *β*-$NaYF_4$:Er, Yb nanoparticles, $YCl_3 \cdot 6H_2O$ (242.69 mg, 0.8 mmol), $YbCl_3 \cdot 6H_2O$ (69.75 mg, 0.18 mmol), and $ErCl_3 \cdot 6H_2O$ (7.64 mg, 0.02 mmol) dissolved in 2 mL deionized water were added to a 100 mL flask containing 7.5 mL oleic acid and 15 mL 1-octadecene. The solution was stirred at room temperature for 0.5 h. Then the mixture was slowly heated to 120 ℃, kept for 1h and then heated to 156 ℃ for another 1 h to get rid of water under argon atmosphere. The system was then cooled down to room temperature. Then 5 mL methanol solution of NH_4F (148.15 mg, 4 mmol) and NaOH (100 mg, 2.5 mmol) was added and the mixture was stirred at room temperature for 2 h. After methanol evaporated, the solution was heated to 280 ℃ and maintained for 1.5 h, then cooled down to room temperature. The resulting product was washed with ethanol and cyclohexane several times, and finally dispersed in cyclohexane for further use. Synthesis of $NaYF_4$:Yb,Tm nanocrystals were performed following a similar protocol by changing the molar ratio of the reagents, $YCl_3 \cdot 6H_2O$ (210.8 mg, 0.695 mmol), $YbCl_3 \cdot 6H_2O$ (116.2 mg, 0.30 mmol), and $TmCl_3 \cdot 6H_2O$ (1.9 mg, 0.005 mmol).

2.2 Surface modification

A ligand exchange process was performed using poly(acrylic acid) (PAA, Mw = 1800) as a multidentate ligand which displaces the original hydrophobic ligands on the UNCPs surface by mixing together 14.5 μl PAA, 1 ml ethanol and 1 mL of UCNPs dispersion in chloroform (15 mg/ml) with overnight stirring. The solution was then centrifuged at 10,000 rpm for 10 min. After being washed 3 times with ethanol and DI water, the particles can be re-dispersed well in water.

3. Ink formulation

3.1 Preparation of hydrophobic printing ink

UCNPs were added into a solution of 90:10 to 70:30 v:v cyclohexane: glycerol trioleate for obtaining ink with optimal performance, such as viscosity and surface tension. The resulting mixture was then stirred for 10 minutes, followed by 10 minutes of sonication, to achieve complete dissolution of nanoparticles.

3.2 Preparation of hydrophilic printing ink

UCNPs after surface modification were added into a solution of 85:15 to 65:35 v:v ethanol-water solution (1:9 v:v ethanol:water):glycerol for obtaining a specific range of dynamic viscosity required for different printers. SDS was then added with a concentration of 3 mg/l to control the surface tension of ink. The resulting mixture was then vigorously stirred for 20 minutes, followed by 20 minutes of sonication, to achieve complete dissolution of nanoparticles.

4. Equipment and characterization

The printing was performed with a modified HP Deskjet 1000 inkjet printer. The dynamic viscosity of inks was measured by a Pinkevitch Viscometer (Shenyangzhongya Glassware Instrument Co., Ltd) with a 0.6 mm diameter and surface tension were measured by capillary tubes (West China University of Medical Science Instrument Factory) with a 0.3 mm diameter. The morphologies of the samples were obtained by using a high-resolution transmission electron microscopy (HRTEM) using a JEM 2100 instrument at an accelerating voltage of 200 kV. The as-prepared samples were characterized by powder X-ray diffraction (XRD) on an XRD-7000 diffractometer with a Cu K_{α} radiation. The FT-IR spectra of the nanoparticles were obtained using a Nicolet iS50 Fourier transform infrared spectrophotometer (Thermo Electron Co., USA) using the KBr method. The upconversion emission spectra were recorded by using a spectrophotometer (QuantaMasterTM40) under external excitation of a 250 mW 980 nm laser diode (RGB Lasersystems). Images of printed patterns upon excitation by a 980 nm CW laser (Changchun Liangli Photoelectric Co., Ltd.) were obtained via a Nikon D90 digital Single Lens Reflex with Macro lens and attached UV/IR filter. All the measurements were performed at room temperature.

Results and discussion

1. β-$NaYF_4$:Yb,Er Nanoparticles

A uniform and high-luminescence pattern requires the ink composed of fluorescent nanoparticles possess good solubility and high luminescence intensity. The $NaYF_4$:Yb,Er nanoparticles used as ink component in this study were synthesized by a thermal decomposition route in the presence of oleic acid (OA) and octadecene, as modified from procedures described previously [38, 39]. To produce two different polar inks, we prepared hydrophobic nanoparticles, OA-UCNPs (**Fig. 2a**), and PAA modified hydrophilic nanoparticles, PAA-UCNPs (**Fig. 2b**). The OA-UCNPs can be easily dispersed in a nonpolar solvent such as cyclohexane, with a mean diameter of 25.8 nm (**Fig. 2a**), which is suitable for smooth printing of this cartridge. The PAA-UCNPs are water-soluble and remain monodispersed with almost unchanged particle size and shape as compared with OA-UCNPs (**Fig. 2a-b**). The XRD pattern of the product shows that all the diffraction peaks can be ascribed to the hexagonal structure of $NaYF_4$ (JCPDS no.16-0334) (**Fig. 2c**). It is reported that hexagonal phase (β-$NaYF_4$:Yb,Er) nanoparticles possess higher upconversion efficiency than cubic phase (α-$NaYF_4$:Yb,Er) ones [40]. And the capping ligands on the surface of UCNPs are identified by FT-IR spectroscopy (**Fig. 2d**). The PAA modified UCNPs samples exhibit a broad band at approximately 3432 cm^{-1}, corresponding to the O-H stretching vibration. The transmission bands at 2924 and 2857 cm^{-1} can be assigned to the asymmetric and symmetric stretching vibrations of the methylene (CH_2) in the long alkyl chain, respectively. Two strong bands centered at 1563 and 1461 cm^{-1} are observed, which can be associated with the asymmetric and symmetric stretching vibrations of carboxylate anions on the surface of the NPs. Meanwhile, the strong band at 1720 cm^{-1} indicates the presence of the COOH groups on the particle surface. Therefore, it can be concluded that PAA have successfully bonded to the UCNPs surface [41]. Further, to generate ink droplets in a controllable manner and to avoid printing instability (*e.g.*, clustering of the particles at the nozzle edge, deviation of the drop trajectory, agglomerates blocking the nozzle), the size of the inks components (*i.e.*, dispersed molecules or nanoparticles) should be less than 1/50 of the nozzle diameter [27]. Here the diameters of nozzles used are over 10 μm, requiring suitable nanoparticle size of less than 200 nm. Therefore, the upconversion nanoparticles we synthesized entirely meet this criteria.

2. Inkjet properties

2.1 Ink properties

To make inks work stably on inkjet printer and optimize the printing resolution and luminescence intensity, we tuned ink properties by evaluating printing performance (*i.e.*, dynamic viscosity and surface tension). When ink drops land on a substrate, the flowage of liquid drops would affect the printing resolution. The spreading of the liquid drops could be measured by the inverse Ohnesorge number, $Z = \sqrt{\gamma\rho\alpha}/\eta$, *i.e.*, nozzle diameter α, and surface tension γ, density ρ, and dynamic viscosity η [31]. To achieve uniform and high-resolution patterns, we adjusted Z ranging between 4.2 and 11.0 for the solvent based printing ink, 5.8 and 13.1 for the aqueous printing ink, which match reported data [27]. Here the dynamic viscosity and surface tension are the critical parameter for printing performance. The dynamic viscosity of ink also affects its flow in the cartridge and through the nozzle, where high viscosity ink may result in nozzle clogging while low viscosity ink may induce damped oscillations in the jet resulting in inhomogeneous droplet size. Besides, low viscosity ink is able to infiltrate through micro pores between fibers of substrates, leading to a situation that only a little ink adheres to the surface of the substrate, thereby decreasing the luminescence intensity of patterns under NIR excitation. In addition, appropriate surface tension of ink helps to keep a relatively small contact angle over substrates, which increases the coverage area for a single drop of ink to form patterns with good uniformity under certain dots per inch (DPI) of a printer. The preferred dynamic viscosity and surface tension of ink for inkjet printer may vary within a specific range at room temperature: the dynamic viscosity varies from 1 to 5 mPa.s (cp) while the surface tension varies from 20 to 60 $mN.m^{-1}$ ($dynes.cm^{-1}$) [42-48].

To prepare ink with preferred parameters mentioned above, we adjusted ink components and their ratios. Organic solvent based or aqueous inks for different substrates were prepared with controlled dynamic viscosity and surface tension. Solvent based ink was prepared with cyclohexane (η equals to 0.886 mpa.s and γ equals to 24.4 mN/m, 25 ℃), which was used to disperse UCNPs, and glycerol trioleate (η equals to 37.8 mpa.s and γ equals to 34.7 mN/m, 25 ℃), which was suitable for preparing a mixture with moderate viscosity and surface tension. The obtained dynamic viscosity and surface tension changes as function of the ratio between cyclohexane and glycerol trioleate (**Fig. 3a-b**). A similar result was obtained from the aqueous printing ink (**Fig. 3c-d**). We dissolved glycerol (η equals to 945 mpa.s and γ equals to 63.3 mN/m, 25 ℃) and SDS into ethanol-water solution (η equals to 1.04 mpa.s and γ equals to 64.8 mN/m, 25 ℃). The obtained dynamic viscosity and surface tension are within the range mentioned above (**Fig. 3c-d**). Compared to previous reported methods [12-14, 16], both the ink components and the preparation procedures are easier for operation and mass production. This demonstrates the advance in using inkjet printer by applying UCNPs for high-throughput security printing.

2.2 Contact angle and spatial resolution

To further optimize the spatial resolution, we controlled the behavior of ejected drop on the substrate, which can be described by fluid dynamics. When a liquid droplet lands on a flat surface, partial wetting results in a finite angle between the liquid and the substrate, known as the contact angle, θ_c [27]. This parameter affects the penetration of ink into substrates which can be described by Washburn's equation: $L = \sqrt{\gamma D t \cos\theta c}/(4\eta)$, where γ is surface tension, D is diameter of capillary tube (capillary porosity between paper fibers), θ_c is contact angle, and η is dynamic viscosity. The quality of printed patterns is mainly affected by different contact angle forming when inks drop on the substrates. Since various substrates possess different capillary porosity and produce different contact angle, studying their influences on patterns printed is essential importance. For this, we printed solvent based and aqueous inks separately onto A4 duplicating and vegetable parchment to demonstrate the relationship between contact angle and the spatial resolution of patterns. The microstructure of the printed papers was analyzed by SEM and was shown in Fig. S1†.

Solvent based and aqueous inks were applied to print a series of parallel lines with equal width and interval. When solvent based and aqueous ink dropped on a piece of A4 duplicating paper (80 g/m^2, white color, purchased from Double A (1991) Public Co., Ltd), they displayed slightly different droplet morphologies which can be reflected by contact angle. After five parallel tests, the contact angle of the solvent based printing ink is 25.7 ±0.8 degrees and the aqueous one is 32.8 ±1.2 degrees (**Fig. 4a-b**). Although a ~21.6% diversity between these two contact angles, printed patterns are of similar spatial resolution as indicated by a series of clear parallel lines of 200 μm equal width and interval (**Fig. 4a-b**). In contrast, when dropping on a piece of vegetable parchment (83 g/m^2, white color, purchased from Suzhouguanhua Paper Factory), there exists a significant variance in the contact angle between two kinds of inks with 9.0 ±0.6 degrees for solvent based ink and 52.7 ±1.3 degrees for aqueous one. As we know, vegetable parchment is hydrophobic, so large contact angle can remain between aqueous ink and vegetable parchment surface, but not the case for solvent based ink. In this situation, the spatial resolution printed using aqueous printing ink is 100-200 μm and solvent based ink is 400-500 μm (**Fig. 4c-d**). In summary, spatial resolution is a directly related of contact angle. Larger contact angle corresponds to higher spatial resolution of printed patterns. As described above, different polarity between ink and substrate facilitates forming of lager contact angle resulting in higher spatial resolution. As compared with solvent based ink, aqueous ink shows higher spatial resolution no matter on A4 paper or on vegetable paper. Aqueous ink is more stable than solvent based ink, and is less apt to block printer holding great potential for further applications.

Compared with screen printing [12, 13] and aerosol jet printer [12, 15, 16], the developed inkjet printing provides higher spatial resolution of smaller than 200 μm (**Fig 4d**). Furthermore, the HP Deskjet 1000 printer applied in this study has its black-and-white DPI of 600×600. Therefore, the spatial resolution can be further improved when using an inkjet printer with higher DPI or using the color cartridge (802 tri-color cartridge). Noteworthy, HP Deskjet 1000 inkjet printer applied in our experiment possesses a theoretical black-and-white printing speed of ~12 pages per minute (PPM) [49], which is faster than other printing techniques studied before in printing complex two-dimensional patterns [12, 16].

3. Luminescence intensity and uniformity

Identification of printed patterns depends mainly on luminescence uniformity which is affected by size and distribution of droplets from the nozzle. Therefore, to verify the luminescence uniformity of printed pattern by our printing system, we tested the variance of the luminescence intensity in a ring printing area with different UCNPs concentrations varied from 0.3 mg/ml to 7.5 mg/ml under 980 nm excitation with power density of ~50 mW/mm^2 (**Fig. 5a**). For each concentration, we randomly tested the luminescence intensity of five points from the printing area. The corresponding luminescence spectrum of UCNPs with different concentrations under 980 nm excitation and the deviation in luminescence intensity peaking at 538 nm were shown in **Fig. 5b-c**. We did not observe significant difference in luminescence intensity (<10% deviation).

4. Application prospect

4.1 Multicolor pattern

When changing the dopant elements types or their ratio, UCNPs are able to emit different colors of light under NIR excitation [50-52]. It is therefore promising to print multicolor anti-counterfeiting patterns using UCNPs. Studies concerning multicolor upconversion luminescence patterns have been reported previously using complex aerosol-jet printer [15]. Here we aimed at demonstrating the easy access of producing multicolor upconversion luminescence patterns using an inkjet printer. We applied two colors of inks composed of UCNPs with different color emission (green, β-$NaYF_4$:Yb,Er and blue, β-$NaYF_4$:Yb,Tm). The printed patterns are shown in **Fig. 6**. Acronym of Xi'an Jiao Tong University patterned by inkjet printer and exposed to 980 nm NIR laser, which "X J" printed with green ink and "T U" with blue ink (**Fig. 6a**). Since these two kinds of inks were able to be printed and excited to display different colors, providing the potential to produce multicolor patterns using different color inks as designed by switching cartridges or using color cartridges of inkjet printer. Moreover, recently there raise a cheap and flexible pattern way, that directly wrote ink on paper using a pen. This method is fitted for simple patterns and patterning various functional materials [53-56]. To further decrease the cost and simplify the progress to a more easy operating way, we directly wrote Chinese characters by a pen filled with two color inks, green and blue. We observed three clear and bright characters on an A4 paper under 980 nm NIR excitation (**Fig. 6c-d**). This design is promising for personalized security information or signature.

4. 2 Double anti-counterfeiting pattern

UV-to-visible downconversion security inks are widely used to produce counterfeit items including identity cards, currency and important documents. However, it always suffers from the appearance of duplications, since UV-to-visible downconversion inks and UV excitation sources have become much easier to obtain. While, the NIR-to-visible upconversion inks and NIR excitation source and reader are more difficult to access. Moreover, the NIR excitation source will not excite standard downconversion luminescence materials, making it possible to print patterns on highly luminescence surface [18]. Therefore, generation of different luminescence patterns that can be excited either by UV or NIR sources will decrease the counterfeit possibility. For this purpose, we applied both UV-to-visible and NIR-to-visible inks for security printing. An A4 paper printed with both NIR-to-visible and UV-to-visible inks was exposed under room light, which was clear that nothing could be identified with naked eyes or cameras (**Fig. 7a**). When excited by a NIR light source, a two-dimensional code was seen clearly without any other interference pattern (**Fig. 7b**). Substitute the NIR light source with an UV light source, a mark 'BEBC' was visualized in the same area, while the two-dimensional code printed using NIR-to-visible ink disappears (**Fig. 7c**).

Conclusions

In summary, we report an easy, fast, multicolor, high-throughput, designable and low cost inkjet printing of upconversion nanoparticles for personal anti-counterfeit and security applications. We synthesized hexagonal phase nanoparticles with high upconversion efficiency and applied them to form two colors printing inks. The dynamic viscosity and surface tension of ink are optimized within a specific range at room temperature. In addition, we found that there was a direct relationship between spatial resolution and contact angle. Larger contact angle contributes to higher spatial resolution of printed patterns. Moreover, the luminescence intensity under the same power density laser excitation can be adjusted by changing the UCNPs concentration in ink, and there was at most 10% deviation in luminescence intensity within a single concentration. Last, we utilized this upconversion luminescence inkjet printing system to print multicolor patterns and double anti-counterfeit patterns, which proves its promising applications for personalized anti-counterfeit and information security. The developed method can make anti-counterfeit marks feasible to produce and hard to duplicate, significantly enhancing the ability of anti-counterfeit.

Acknowledgements

This work was financially supported by the National Natural Science Foundation of China (11120101002), International Science & Technology Cooperation Program of China (2013DFG02930), National Key Scientific Apparatus Development of Special Item (2013YQ190467), the Fundamental Research Funds for the Central Universities (2012jdhz46). Min Lin is supported by scholarship from the China Scholarship of Council. Feng Xu was also partially supported by the China Young 1000-Talent Program and the Program for New Century Excellent Talents in University. The TEM work was done at International Center for Dielectric Research (ICDR), Xi'an Jiaotong University, Xi'an, China. The authors also thank Ms. Lu Lu and Mr. Ma Chuan Sheng for their help in using TEM.

Notes and references

[a] The Key Laboratory of Biomedical Information Engineering of Ministry of Education, School of Life Science and Technology, Xi’an Jiaotong University, Xi’an 710049, P.R. China. *E-mail: fengxu@mail.xjtu.edu.cn*

[b] Bioinspired Engineering and Biomechanics Center (BEBC), Xi’an Jiaotong University, Xi’an 710049, P.R. China. *E-mail: minlin@mail.xjtu.edu.cn*

[c] School of Energy and Power Engineering, Xi’an Jiaotong University, Xi’an 710049, P.R. China.

[d] College of Life Sciences, Nanjing Agricultural University, Nanjing 210095, P.R. China.

[e] Center for Sarcoma and Connective Tissue Oncology, Massachusetts General Hospital, Harvard Medical School, MA 02114, USA.

* The authors contributed equally

† Electronic Supplementary Information (ESI) available: SEM micrograph of A4 duplicating paper and vegetable parchment paper printed with(out) solvent based ink and aqueous ink. See DOI: 10.1039/b000000x/

References

1. Yoon B, Lee J, Park IS, Jeon S, Lee J, Kim J-M. Recent functional material based approaches to prevent and detect counterfeiting. Journal of Materials Chemistry C. 2013; **1**(13): 2388-403.

2. Liu Y, Ai K, Lu L. Designing lanthanide-doped nanocrystals with both up- and down-conversion luminescence for anti-counterfeiting. Nanoscale. 2011; **3**(11): 4804-10.

3. Cui Y, Hegde RS, Phang IY, Lee HK, Ling XY. Encoding molecular information in plasmonic nanostructures for anti-counterfeiting applications. Nanoscale. 2014; **6**(1): 282-8.

4. Jin T, Meng W, Yan S, Zhao M. Method for producing laser hologram anti-counterfeit mark with identifying card and inspecting card and inspecting apparatus for the mark. Google Patents; 1999.

5. Yushun Y, Xiangming H, Quanrong Z. Breakthrough in fake prevention. Nuclear track-etching. PHYSICS. 1999.

6. Andres J, Hersch RD, Moser J-E, Chauvin A-S. A New Anti-Counterfeiting Feature Relying on Invisible Luminescent Full Color Images Printed with Lanthanide-Based Inks. Advanced Functional Materials. 2014: n/a-n/a.

7. Kumar P, Dwivedi J, Gupta BK. Highly-luminescent dual mode rare-earth nanorods assisted multi-stage excitable security ink for anti-counterfeiting applications. Journal of Materials Chemistry C. 2014.

8. Cadarso VJ, Chosson S, Sidler K, Hersch RD, Brugger J. High-resolution 1D moires as counterfeit security features. Light Sci Appl. 2013; **2**: e86.

9. Gupta BK, Haranath D, Saini S, Singh VN, Shanker V. Synthesis and characterization of ultra-fine Y2O3:Eu3+ nanophosphors for luminescent security ink applications. Nanotechnology. 2010; **21**(5): 055607.

10. Anh TK, Loc DX, Huong TT, Vu N. Luminescent nanomaterials containing rare earth ions for security printing. International Journal of Nanotechnology. 2011; **8**(3): 335-46.

11. Sangeetha NM, Moutet P, Lagarde D, Sallen G, Urbaszek B, Marie X, et al. 3D assembly of upconverting NaYF4 nanocrystals by AFM nanoxerography: creation of anti-counterfeiting microtags. Nanoscale. 2013; **5**(20): 9587-92.

12. Blumenthal T, Meruga J, Stanley May P, Kellar J, Cross W, Ankireddy K, et al. Patterned direct-write and screen-printing of

NIR-to-visible upconverting inks for security applications. Nanotechnology. 2012; **23**(18): 185305.

13. Cross W, Blumenthal T, Kellar J, May PS, Meruga J, Luu Q. Rare-Earth Doped Nanoparticles in Security Printing Applications. MRS Proceedings. 2012; **1471**.

14. Kim WJ, Nyk M, Prasad PN. Color-coded multilayer photopatterned microstructures using lanthanide (III) ion co-doped NaYF4 nanoparticles with upconversion luminescence for possible applications in security. Nanotechnology. 2009; **20**(18): 185301.

15. Meruga JM, Baride A, Cross W, Kellar JJ, May PS. Red-green-blue printing using luminescence-upconversion inks. Journal of Materials Chemistry C. 2014; **2**(12): 2221-7.

16. Meruga JM, Cross WM, Stanley May P, Luu Q, Crawford GA, Kellar JJ. Security printing of covert quick response codes using upconverting nanoparticle inks. Nanotechnology. 2012; **23**(39): 395201.

17. Bao Y, Luu QAN, Zhao Y, Fong H, May PS, Jiang C. Upconversion polymeric nanofibers containing lanthanide-doped nanoparticles via electrospinning. Nanoscale. 2012; **4**(23): 7369-75.

18. Ma R, Bullock E, Maynard P, Reedy B, Shimmon R, Lennard C, et al. Fingermark detection on non-porous and semi-porous surfaces using NaYF< sub> 4</sub>: Er, Yb up-converter particles. Forensic science international. 2011; **207**(1): 145-9.

19. Zhao J, Jin D, Schartner EP, Lu Y, Liu Y, Zvyagin AV, et al. Single-nanocrystal sensitivity achieved by enhanced upconversion luminescence. Nat Nano. 2013; **8**(10): 729-34.

20. Zhao J, Lu Z, Yin Y, McRae C, Piper JA, Dawes JM, et al. Upconversion luminescence with tunable lifetime in NaYF4:Yb,Er nanocrystals: role of nanocrystal size. Nanoscale. 2013; **5**(3): 944-52.

21. Lu Y, Zhao J, Zhang R, Liu Y, Liu D, Goldys EM, et al. Tunable lifetime multiplexing using luminescent nanocrystals. Nat Photon. 2014; **8**(1): 32-6.

22. Sirringhaus H, Kawase T, Friend RH, Shimoda T, Inbasekaran M, Wu W, et al. High-Resolution Inkjet Printing of All-Polymer Transistor Circuits. Science. 2000; **290**(5499): 2123-6.

23. Kim HS, Kang JS, Park JS, Hahn HT, Jung HC, Joung JW. Inkjet printed electronics for multifunctional composite structure. Composites Science and Technology. 2009; **69**(7-8): 1256-64.

24. Tseng H-Y, Purushothaman B, Anthony J, Subramanian V. High-speed organic transistors fabricated using a novel hybrid-printing technique. Organic Electronics. 2011; **12**(7): 1120-5.

25. Tseng H-Y, Subramanian V. All inkjet-printed, fully self-aligned transistors for low-cost circuit applications. Organic Electronics. 2011; **12**(2): 249-56.

26. Perelaer J, Abbel R, Wünscher S, Jani R, van Lammeren T, Schubert US. Roll-to-Roll Compatible Sintering of Inkjet Printed Features by Photonic and Microwave Exposure: From Non-Conductive Ink to 40% Bulk Silver Conductivity in Less Than 15 Seconds. Advanced Materials. 2012; **24**(19): 2620-5.

27. Torrisi F, Hasan T, Wu W, Sun Z, Lombardo A, Kulmala TS, et al. Inkjet-Printed Graphene Electronics. ACS Nano. 2012; **6**(4): 2992-3006.

28. Song KW, Costi R, Bulovic V. Electrophoretic Deposition of CdSe/ZnS Quantum Dots for Light-Emitting Devices. Advanced Materials. 2013; **25**(10): 1420-3.

29. Böberl M, Kovalenko MV, Gamerith S, List EJW, Heiss W. Inkjet-Printed Nanocrystal Photodetectors Operating up to 3 μm Wavelengths. Advanced Materials. 2007; **19**(21): 3574-8.

30. Haverinen HM, Myllylä RA, Jabbour GE. Inkjet Printed RGB Quantum Dot-Hybrid LED. J Display Technol. 2010; **6**(3): 87-9.

31. Finn DJ, Lotya M, Cunningham G, Smith RJ, McCloskey D, Donegan JF, et al. Inkjet deposition of liquid-exfoliated graphene and MoS2 nanosheets for printed device applications. Journal of Materials Chemistry C. 2014; **2**(5): 925-32.

32. Hernandez-Sosa G, Tekoglu S, Stolz S, Eckstein R, Teusch C, Trapp J, et al. The compromises of printing organic electronics: a case study of gravure-printed light-emitting electrochemical cells. Adv Mater. 2014; **26**(20): 3235-40.

33. Minxuan K, Jingxia W, Bin B, Fengyu L, Libin W, Lei J, et al. Inkjet Printing Patterned Photonic Crystal Domes for Wide Viewing-Angle Displays by Controlling the Sliding Three Phase Contact Line. Adv Opt Mater. 2014; **2**(1): 34-8.

34. Abe K, Suzuki K, Citterio D. Inkjet-Printed Microfluidic Multianalyte Chemical Sensing Paper. Analytical Chemistry. 2008; **80**(18): 6928-34.

35. Dua V, Surwade SP, Ammu S, Agnihotra SR, Jain S, Roberts KE, et al. All-organic vapor sensor using inkjet-printed reduced graphene oxide. Angewandte Chemie. 2010; **49**(12): 2154-7.

36. Yu WW, White IM. Inkjet-printed paper-based SERS dipsticks and swabs for trace chemical detection. Analyst. 2013; **138**(4): 1020-5.

37. Park J-U, Hardy M, Kang SJ, Barton K, Adair K, Mukhopadhyay Dk, et al. High-resolution electrohydrodynamic jet printing. Nat Mater. 2007; **6**(10): 782-9.

38. Fan W, Shen B, Bu W, Chen F, Zhao K, Zhang S, et al. Rattle-Structured Multifunctional Nanotheranostics for Synergetic Chemo-/Radiotherapy and Simultaneous Magnetic/Luminescent Dual-Mode Imaging. Journal of the American Chemical Society. 2013; **135**(17): 6494-503.

39. Qian H-S, Zhang Y. Synthesis of Hexagonal-Phase Core−Shell NaYF4 Nanocrystals with Tunable Upconversion Fluorescence. Langmuir. 2008; **24**(21): 12123-5.

40. Wang F, Liu X. Recent advances in the chemistry of lanthanide-doped upconversion nanocrystals. Chemical Society Reviews. 2009; **38**(4): 976-89.

41. Wu S, Duan N, Ma X, Xia Y, Wang H, Wang Z. A highly sensitive fluorescence resonance energy transfer aptasensor for staphylococcal enterotoxin B detection based on exonuclease-catalyzed target recycling strategy. Analytica Chimica Acta. 2013; **782**(0): 59-66.

42. de Gans B-J, Schubert US. Inkjet Printing of Polymer Micro-Arrays and Libraries: Instrumentation, Requirements, and Perspectives. Macromolecular Rapid Communications. 2003; **24**(11): 659-66.

43. Lee HH, Chou KS, Huang KC. Inkjet printing of nanosized silver colloids. Nanotechnology. 2005; **16**(10): 2436-41.

44. Mei J, Lovell MR, Mickle MH. Formulation and processing of novel conductive solution inks in continuous inkjet printing of 3-D electric circuits. Electronics Packaging Manufacturing, IEEE Transactions on. 2005; **28**(3): 265-73.

45. Saunders RE, Gough JE, Derby B. Delivery of human fibroblast cells by piezoelectric drop-on-demand inkjet printing. Biomaterials. 2008; **29**(2): 193-203.

46. Son Y, Kim C. Spreading of inkjet droplet of non-Newtonian fluid on solid surface with controlled contact angle at low Weber and Reynolds numbers. Journal of Non-Newtonian Fluid Mechanics. 2009; **162**(1-3): 78-87.

47. Son Y, Kim C, Yang DH, Ahn DJ. Spreading of an inkjet droplet on a solid surface with a controlled contact angle at low Weber and Reynolds numbers. Langmuir. 2008; **24**(6): 2900-7.

48. Xu D, Sanchez-Romaguera V, Barbosa S, Travis W, de Wit J, Swan P, et al. Inkjet printing of polymer solutions and the role of chain entanglement. Journal of Materials Chemistry. 2007; **17**(46): 4902.

49. contributors W. HP Deskjet. 11 March 2014 07:31 UTC [cited; Available from: http://en.wikipedia.org/w/index.php?title=HP_Deskjet&oldid=599100789

50. Wang F, Liu X. Upconversion Multicolor Fine-Tuning: Visible to Near-Infrared Emission from Lanthanide-Doped NaYF4 Nanoparticles. Journal of the American Chemical Society. 2008; **130**(17): 5642-3.

51. Ni D, Bu W, Zhang S, Zheng X, Li M, Xing H, et al. Single Ho3+-Doped Upconversion Nanoparticles for High-Performance T2-Weighted Brain Tumor Diagnosis and MR/UCL/CT Multimodal Imaging. Advanced Functional Materials. 2014: n/a-n/a.

52. Ni D, Zhang J, Bu W, Xing H, Han F, Xiao Q, et al. Dual-Targeting Upconversion Nanoprobes across the Blood-Brain Barrier for Magnetic Resonance/Fluorescence Imaging of Intracranial Glioblastoma. ACS Nano. 2014.

53. Han YL, Hu J, Genin GM, Lu TJ, Xu F. BioPen: direct writing of functional materials at the point of care. Sci Rep. 2014; **4**.

54. Tian L, Tadepalli S, Farrell ME, Liu K-K, Gandra N, Pellegrino PM, et al. Multiplexed charge-selective surface enhanced Raman scattering based on plasmonic calligraphy. Journal of Materials Chemistry C. 2014; **2**(27): 5438-46.

55. Russo A, Ahn BY, Adams JJ, Duoss EB, Bernhard JT, Lewis JA. Pen-on-Paper Flexible Electronics. Advanced Materials. 2011; **23**(30): 3426-30.

56. Mirica KA, Weis JG, Schnorr JM, Esser B, Swager TM. Mechanical Drawing of Gas Sensors on Paper. Angewandte Chemie International Edition. 2012; **51**(43): 10740-5.

Figures:

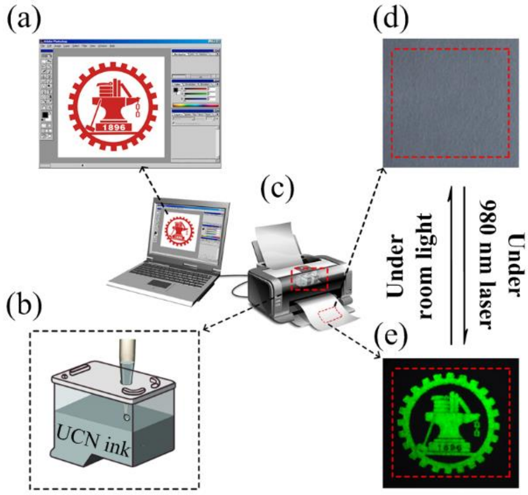

Figure. 1 Schematic of inkjet printing upconversion nanoparticles for anti-counterfeit applications. (a) Designing patterns on the computer using software. (b) Preparing the cartridge and UCNPs ink. (c) Printing patterns using the inkjet printer connected with the computer. (d) Upconverting patterns exposed under room light. (e) Upconverting patterns exposed under 980 nm laser.

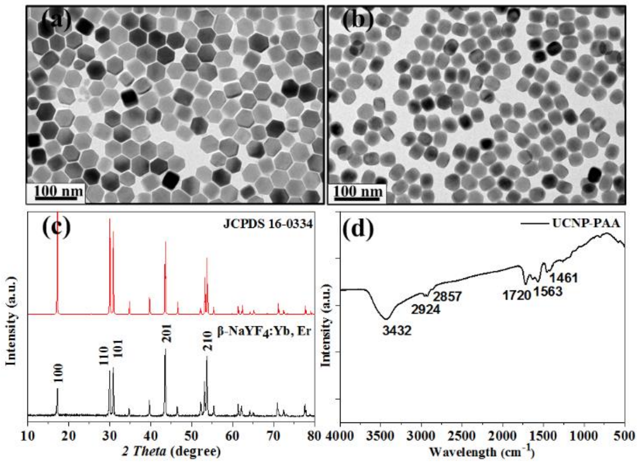

Figure. 2 Characterization of the UCNPs. TEM image of β-$NaYF_4$:Er,Yb nanoparticles (a) before and (b) after PAA modification. (c) Powder XRD of β-$NaYF_4$:Er,Yb nanocrystal sample compared to ICDD PDF card for β-$NaYF_4$. (d) FT-IR spectrum of PAA capped β-$NaYF_4$:Er,Yb.

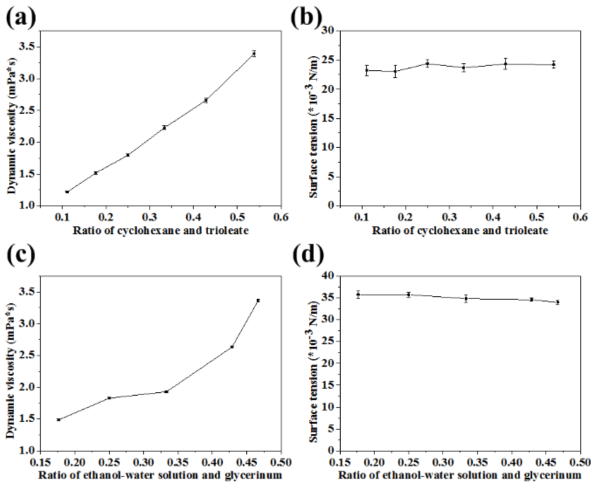

Figure. 3 Characterization of the UCNPs ink with varying ratios of components at 25±1℃. (a) The dynamic viscosity of solvent based printing ink changes with v:v cyclohexane : glycerol trioleate ratio. (b) The gas-liquid surface tension of solvent based printing ink changes with v:v cyclohexane : glycerol trioleate ratio. (c) The dynamic viscosity of aqueous printing ink changes with v:v ethanol-water solution(10%) : glycerol ratio. (d) The gas-liquid surface tension of aqueous printing ink changes with v:v ethanol-water solution(10%) : glycerol ratio.

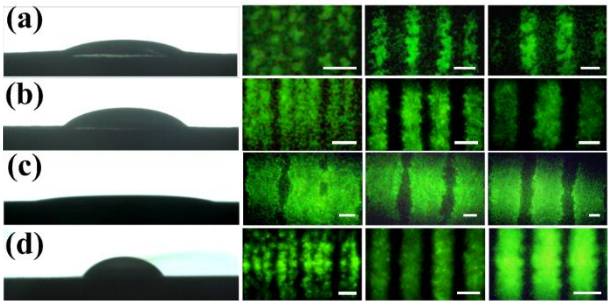

Figure. 4 Characterization of the spatial resolution of printing. (a) Droplet morphology of solvent based printing ink on A4 duplicating paper and equal interval and width (from left to right, 100 μm, 200 μm, 300 μm) lines printed. (b) Droplet morphology of aqueous printing ink on A4 duplicating paper and equal interval and width (from left to right, 100 μm, 200 μm, 300 μm) lines printed. (c) Droplet morphology of solvent based printing ink on vegetable parchment and equal interval and width (from left to right, 400 μm, 500 μm, 600 μm) lines printed. (d) Droplet morphology of aqueous printing ink on vegetable parchment and equal interval and width (from left to right, 100 μm, 200 μm, 300 μm) lines printed. The scale bar of each represents 300 μm.

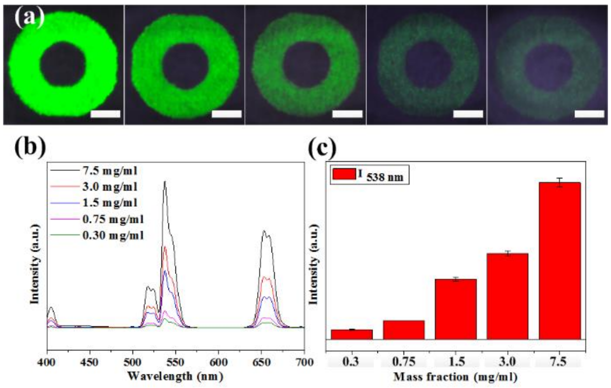

Figure. 5 Characterization of luminescence intensity and uniformity. (a) Luminescence changes along with the change of the UCNPs concentration (from left to right 7.5 mg/ml, 3.0 mg/ml, 1.5 mg/ml, 0.75 mg/ml, 0.3 mg/ml). Patterns are exploded under 980nm laser, with power density of ~50 mW/mm^2. Figures are obtained using Nikon D90 camera under f 5.8 (aperture) and 6 s (shutter duration) condition. (b) Luminescence spectrum of different mass fractions of UCNPs. (c) Variance of luminescence intensity in 538 nm wavelength of ring printing areas with different mass fractions of UCNPs. The scale bar of each represents 2 mm.

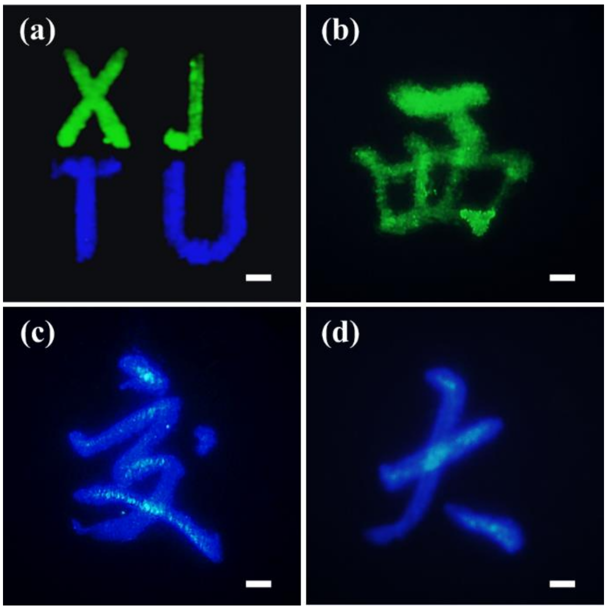

Figure. 6 Multicolor patterning of $NaYF_4$:Yb,Er (green) and $NaYF_4$:Yb,Tm (blue) by direct-writing with pen. (a) Printed acronym of Xi'an Jiao Tong University, which "X J" printed with green ink and "T U" with blue ink. (b)Write with green ink and (c)-(d) with blue ink. All picture obtained under 980 nm NIR laser source. The scale bar represents 1 mm.

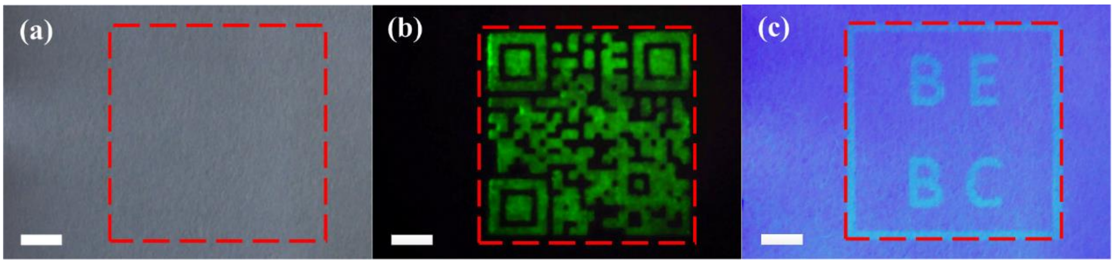

Figure. 7 Double anti-counterfeiting pattern. (a) Area of both NIR-to-visible and UV-to-visible printing features. (b) Two-dimension code printed using NIR-to-visible upconversion ink. (c) 'BEBC' mark printed using UV-to-visible downconversion ink. The scale bar represents 2 mm.